

This document is confidential and is proprietary to the American Chemical Society and its authors. Do not copy or disclose without written permission. If you have received this item in error, notify the sender and delete all copies.

**Water and Membrane Dynamics in Suspensions of Lipid Vesicles Functionalized with Polyethylene Glycols**

Journal:	<i>The Journal of Physical Chemistry</i>
Manuscript ID:	jp-2013-10894x.R2
Manuscript Type:	Article
Date Submitted by the Author:	06-May-2014
Complete List of Authors:	Clop, Eduardo; Universidad Nacional de Córdoba, Química; IIBYT (CONICET-UNC), Chattah, Ana; FaMAF, Perillo, Maria; Universidad Nacional de Córdoba, Química

SCHOLARONE™  
Manuscripts

1  
2  
3  
4  
5  
6  
7  
8 Water and Membrane Dynamics in Suspensions of Lipid Vesicles  
9  
10 Functionalized with Polyethylene Glycols.  
11  
12  
13  
14

15 Eduardo M. Clop<sup>1</sup>, Ana K. Chattah<sup>2</sup> and María A. Perillo<sup>1\*</sup>  
16  
17  
18  
19

20  
21 <sup>1</sup>IIByT (CONICET-UNC). Cátedra de Química Biológica, Facultad de Ciencias Exactas  
22 Físicas y Naturales, Universidad Nacional de Córdoba. Av. Vélez Sarsfield 1611,  
23 X5016GCA Córdoba, Argentina.  
24  
25

26  
27 <sup>2</sup>Facultad de Matemática Astronomía y Física (FaMAF) and IFEG (CONICET-UNC).  
28 Ciudad Universitaria, X5016LAE Córdoba, Argentina.  
29  
30  
31

32  
33  
34  
35  
36  
37 \* Corresponding author

38  
39 <sup>1</sup>IIByT (CONICET-UNC). Cátedra de Química Biológica, Facultad de Ciencias Exactas  
40 Físicas y Naturales, Universidad Nacional de Córdoba. Av. Vélez Sarsfield 1611,  
41 X5016GCA Córdoba, Argentina. [mperillo@efn.uncor.edu](mailto:mperillo@efn.uncor.edu)  
42  
43

44  
45 FAX: + 54-351-4334139, e-mail:  
46  
47  
48  
49  
50  
51  
52  
53  
54  
55

Field Code Changed

## Abstract

The present work was aimed at studying the molecular dynamics at different levels of model membranes having a simulated glycoflic, with focus on the molecular crowding conditions at the lipid-water interfacial region. So, binary mixtures of dipalmitoylphosphatidylcholine (dpPC) and a polyethylene glycol (PEG<sup>n</sup>) derivative of dipalmitoylphosphatidylethanolamine (PE) (where  $n=350, 1000$  and  $5000$ , respectively, refers to PEGs molecular masses) were submitted to <sup>1</sup>H spin-lattice relaxation time ( $T_1$ ) and <sup>31</sup>P NMR spectra analysis.

<sup>1</sup>H NMR relaxation times revealed two contributing components in each proton system (PEG, phospholipids and water), for all the mixtures studied, exhibiting values of  $T_1$  with very different orders of magnitude. This allowed identifying confined and bulk water populations as well as PEG moieties becoming more disordered and independent from the phospholipid moiety as  $n$  increased. <sup>31</sup>P spectra showed a typical broad bilayer signal for  $n=350$  and  $1000$ , and an isotropic signal characteristic of micelles for  $n=5000$ . Surface pressure ( $\pi$ ) - molecular area isotherms and compressional modulus measurements provided further structural information. Moreover, Epifluorescence Microscopy data from monolayers at  $\pi \sim 30$  mN/m, the expected equilibrium  $\pi$  in lipid bilayers, allowed us to postulate that both <sup>1</sup>H populations resolved through NMR in phospholipids and lipopolymers corresponded to different phase domains.

**Keywords:** polymer grafted lipids; PE-PEG; water dynamics.

Formatted: English (U.S.)

**Abbreviations**

FID, free induction decay; NMR, nuclear magnetic resonance; PEG, poly(ethylene glycol); [PEG], poly(ethylene glycol) concentration; GC, Glycocalix; dpPC, dipalmitoylphosphatidylcholine; HC, hydrocarbon chain;  $^1\text{H}$ , proton; MLVs, multi-lamellar vesicles; PE, dipalmitoylphosphatidylethanolamine; PH, polar head;  $T_1$ , spin-lattice relaxation time;  $T_{1A}^X$ ,  $T_{1B}^X$ , long and short relaxation time components in the X peak (Bruker 400 MHz experiment) (where X= PEG, H<sub>2</sub>O, HC or PH).

## Introduction

Biochemical processes occur at a high global concentration of macromolecules, between 50 and 400 mg/ml (5 - 40% W/V)<sup>1-3</sup>. This is a distinguishing feature of living systems usually described as molecular crowded (MC) environments. Within MC media, macromolecules occupy a large fraction of volume that cannot be occupied by other molecules<sup>4</sup>. So, large molecules are confined due to their big size compared with the pore size<sup>5, 6</sup> and the volume accessible to small molecules is significantly lower than in conditions of dilute solutions, where most of experiments are done. As a result, molecules are subjected to steric and diffusional restrictions affecting their properties<sup>7</sup>. Moreover, in MC systems a significant population of water molecules remain tightly bound to the crowding species thus being sequestered from bulk solvent<sup>8</sup>.

The cellular glycocalix (GC) is a typical example of MC environment. The GC is a polysaccharide protective layer that conforms the environment where membrane anchored proteins are embedded<sup>9, 10</sup>. It contributes to the antiadhesive properties of cells under normal disease free conditions and may also control the accessibility of solutes (e.g. drugs) to the cell interior and hinder the binding of targeted carriers to the cell surface<sup>11</sup>. The compactness of the GC is expected to affect its structure and hydration conditions. Consequently, studies on water dynamics within the molecular crowded environment of a GC would be of utmost importance to understand physical and biochemical phenomena taking place at the membrane interfacial region.

In this regard, Nuclear Magnetic Resonance (NMR) through spin-lattice and spin-spin relaxation times has proven to be a very useful technique to provide information of aqueous solutions, on a variety of time scales and solute concentrations<sup>12-15</sup>. In addition, it is a noninvasive method that can be applied to a wide spectrum of solution samples. In particular,

Field Code Changed

Field Code Changed

Field Code Changed

Field Code Changed

Field Code Changed

Field Code Changed

Field Code Changed

Field Code Changed

1  
2  
3  
4  
5  
6  
7 it has allowed identify the dynamics of different water populations, helping to distinguish free  
8 liquid fractions from structured water in the presence of solutes<sup>16</sup>. Additionally, 1D <sup>31</sup>P-  
9 NMR spectra have been extensively used to study the coexistence of different types of  
10  
11  
12  
13  
14  
15  
16  
17  
18  
19  
20  
21  
22  
23  
24  
25  
26  
27  
28  
29  
30  
31  
32  
33  
34  
35  
36  
37  
38  
39  
40  
41  
42  
43  
44  
45  
46  
47  
48  
49  
50  
51  
52  
53  
54  
55  
56  
57  
58  
59  
60

Using polyethylene glycol (PEG) in solution, it is possible to achieve MC conditions<sup>4</sup>.  
19, 20. The ability of PEG to fulfill this role has been attributed mainly to its physical  
properties, such as solubility in water at all concentrations, a large exclusion volume and a  
high degree of conformational entropy<sup>21-23</sup>. Recently, from NMR measurements of spin-  
lattice relaxation times of PEG<sup>6000</sup> solutions, we reported the presence of two molecular  
populations, both in water and in PEG as well as a PEG<sup>6000</sup> aggregation also supported by  
dynamic light scattering data<sup>24</sup>. However, this model system cannot reproduce the anisotropy  
and molecular orientation encountered at an interface<sup>1-3</sup>. So, lipids covalently modified with  
hydrophilic polymers, e.g. glycolipids with both linear and branched head groups, have been  
considered good candidates to build up a model GC<sup>25, 26</sup>. Additionally, lipopolymers  
containing polyethyleneglycol (PEG) have been widely used in liposome formulation for  
drug encapsulation and transport<sup>27</sup>. In these systems, PEG chains form an interfacial  
hydrophilic layer that prevents aggregation and nonspecific binding<sup>28</sup>. From both a  
fundamental and practical point of view, it is of interest to investigate the phase and  
aggregation behavior of PEG-lipid/phospholipid mixtures<sup>29</sup>.

In the present work we study the water dynamics in vesicles suspensions composed of  
binary mixtures of dipalmitoylphosphatidylcholine (dpPC) and derivatives of  
dipalmitoylphosphatidylethanolamine (PE) modified with a PEG moiety.: dpPC/PE-PEG<sup>n</sup>  
(9:1 mol%), where *n* is the molar mass (350, 1000 or 5000 Da) corresponding to PEGs with 7,  
23 and 113 ethylene residues, respectively (see molecular structures in Figure 1). This gave  
the possibility of controlling the thickness of the hydrophilic interfacial region, by varying the

1  
2  
3  
4  
5  
6  
7 components in the mixture. The molecular dynamics was analyzed using NMR techniques, in  
8 particular  $^1\text{H}$  spin-lattice relaxation times ( $T_1$ ) and  $^{31}\text{P}$  spectra. Measurements on  $\pi$ -Mma  
9 isotherm and compressional modulus measurements provided further structural information  
10 on these systems.  
11  
12  
13

## 14 15 16 **Materials and Methods**

### 17 18 **Materials**

19  
20 1,2-dipalmitoyl-*sn*-glycero-3-phosphoethanolamine-N-[methoxy(polyethyleneglycol)  
21 with PEGs average molecular masses of 350, 1000 and 5000 (PE-PEG<sup>350</sup>, PE-PEG<sup>1000</sup>, PE-  
22 PEG<sup>5000</sup>, respectively) and 1,2-dipalmitoyl-*sn*-glycero-3-phosphocholine (dpPC) were  
23 purchased from Avanti Polar Lipids (Alabaster, Alabama), Dil C<sub>18</sub>, 1,1'-dioctadecyl-3,3',3'-  
24 tetramethylindocarbocyanine perchlorate was from Molecular probes Inc. (Eugene, OR,  
25 USA) and virgin deuterated water was kindly donated by Central Nuclear Embalse de Río  
26 Tercero, Córdoba, Argentina.  
27  
28  
29  
30  
31  
32  
33

Formatted: English (U.S.)

### 34 35 **Methods**

#### 36 37 38 **Membrane preparation**

39  
40 Scheme 1 displays the dpPC/PE-PEG<sup>n</sup> systems for n= 350, 1000 and 5000 prepared as  
41 follows. Stock solutions of the pure compounds were mixed in the appropriate proportion  
42 (dpPC : dpPE-PEG (9:1) molar ratio) in chloroform:methanol (2:1); then, the solvent was  
43 evaporated under a nitrogen stream. In a previous work, through the Langmuir Film balance  
44 technique, we studied the mixing behavior of dpPC/PE-PEG<sup>n</sup> finding that the thin films  
45 containing PE-PEG<sup>1000</sup> or PE-PEG<sup>5000</sup> formed stable monolayers in mixtures with dpPC up to  
46 a lipopolymer molar fraction x= 0.2, and up to x=0.1 in the case of PE-PEG<sup>350</sup>.  
47  
48  
49  
50  
51  
52  
53  
54

Field Code Changed

1  
2  
3  
4  
5  
6  
7 The film thus formed was left under vacuum for no less than 2 h to remove residual  
8 solvent. Lipids were re-suspended to reach 20 mM concentration in deuterated water at 50 °C,  
9 by 3 min. vortexing to form multi-lamellar vesicles (MLVs) The MLVs suspension was tip  
10 sonicated for 45 min using a SonaBox Ultrasonic Homogenizer 150 VT (Biologics Inc.,  
11 Manassas, VA, USA) to obtain Small Unilamellar Vesicles (SUV). Alternating cycles of  
12 sonication and rest (30 sec) were made in an ice water bath to keep the temperature between  
13 0-4 °C. Samples were then centrifuged at 10,000 g for about 20 min. to remove any residual  
14 large particles and titanium released from the sonicator tip. The SUVs were used in all <sup>1</sup>H-  
15 NMR and <sup>31</sup>P-NMR experiments.  
16  
17  
18  
19  
20  
21  
22  
23  
24  
25

### 26 NMR experiments

27  
28 <sup>1</sup>H spin-lattice relaxation times (T<sub>1</sub>) were measured for all the systems in a Bruker  
29 Avance 400 MHz using the inversion recovery (IR) pulse sequence( $\pi-t-\pi/2$ -Acquisition) <sup>31</sup>  
30 Liposomes were dispersed in D<sub>2</sub>O containing trace amounts of H<sub>2</sub>O. Then, separated  
31 resonances belonging to <sup>1</sup>H nucleus in phospholipids, PEG moiety from lipopolymers and  
32 H<sub>2</sub>O were observed, enabling the spectral resolution of proton signals belonging to different  
33 parts of the system. The recovery times in the IR experiments *t* ranged between 10 μs and  
34 128 s.  
35  
36  
37  
38  
39  
40

41  
42 <sup>31</sup>P-NMR spectra for all the systems were measured at 121.49 MHz <sup>31</sup>P frequency on  
43 a Bruker Avance 300 MHz spectrometer. These spectra were obtained performing a  $\pi/2$  pulse  
44 of 9.4 μs with <sup>1</sup>H decoupling during acquisition with a proton field of 60 kHz. Recycling time  
45 was 4 s and 6000 scans were accumulated for each sample.  
46  
47  
48

49 All the NMR experiments were performed at 37°C in order to emulate the biological  
50 conditions.  
51  
52  
53  
54  
55



### $\pi$ -Mma isotherm recording

Surface pressure-mean molecular area compression isotherms were obtained for pure or mixed lipid monolayers as described before at different surface pressures <sup>32</sup>. Briefly, experiments were performed at  $37 \pm 1$  °C, with a Minitrough II (KSV Instruments Ltd., Finland) enclosed in an acrylic box to avoid surface contamination, which measured the surface pressure ( $\pi$ ) with the Wilhelmy plate method. The absence of surface-active compounds in the pure solvents and in the subphase solution was routinely checked before each run by reducing the available surface area to less than 10% of its original value, after allowing enough time for the adsorption of possible impurities that might have been present in trace amounts.

The lipid mixture was dissolved in chloroform-methanol (2:1V/V) and spread on the air-water surface. After the solvent evaporation and the monolayer stabilization the interface was compressed at a constant rate of 10 mm/min. A lower compression rate ( $1 \text{ mm}\cdot\text{min}^{-1}$ ) was tested with identical results.  $\pi$  and molecular area ( $A$ ) were registered during the process with a precision within  $\pm 1 \text{ mN/m}$  and  $\pm 0.01 \text{ nm}^2$ , respectively. From the  $\pi$ - $A$  isotherms the surface parameters, minimum molecular area,  $A_{\text{min}}$ , and collapse pressure,  $\pi_c$ , were obtained.  $A_{\text{min}}$  is the minimum area occupied by an amphipathic molecule in a monolayer at the closest molecular packing, and the collapse pressure  $\pi_c$ , is the maximal  $\pi$  that correspond to  $A_{\text{min}}$ . The latter parameter is related to monolayer stability and can be associated with intermolecular cohesion forces of the amphipathic molecules, the affinity of the polar groups for the aqueous subphase and the optimal hydrophobic-hydrophilic balance in the molecule.

Isotherms shown in Fig. 6 are typical examples with high overall reproducibility (e.g. errors in area measurements ranged between 3 and 5%).

Field Code Changed

Formatted: Not Highlight

### Compressional modulus

The compressional modulus  $K$  was calculated for each isotherm according to Eq.2:

$$K = -\left(A_{\pi}\right)\left(\frac{\delta\pi}{\delta A}\right)_T \quad [1]$$

where  $A$  is the mean molecular area (Mma).  $K$  allows inferring about the elasticity of the monolayer, and to define more precisely the bidimensional phase transitions from the  $\pi$ -Mma isotherm profile.

For ideal mixtures with a defined composition, an ideal  $K$  ( $K_{id}$ ) was calculated as the weighted sum of the reciprocals of the compressibilities for individual monolayer components ( $1/C_i$ ) using the molar fraction ( $x_i$ ) as the weighting factor, according to eqs.2 and 3.

$$K_{id} = \sum x_i \cdot \frac{1}{C_i} \quad [2]$$

$$C_i = -\left(\frac{1}{A_i}\right)\left(\frac{\delta A_i}{\delta\pi}\right)_T \quad [3]$$

### Epifluorescence Microscopy

Epifluorescence microscopy (EFM) was performed as described previously<sup>33</sup>. Pure lipid monolayers were doped with 1 – 2 mol % of DiI-C<sub>18</sub> and observed with an inverted epifluorescence microscope directly from the interface. Briefly, a KSV Minisystem surface barostat was mounted on the stage of a Nikon Eclipse TE2000-U (Tokyo, Japan) microscope, which was supplied with 209 extra large working distance optics. The Teflon trough used had a 35-mm diameter quartz window at its base, which allowed the observation of the monolayer through the trough. The monolayer morphology was documented with a color video camera Nikon DS-5 M with a supported resolution up to 2,560–1,920 pix (Capture).

Field Code Changed

Field Code Changed

**Dynamic light scattering (DLS)**

Aqueous dispersion of dpPC/PE-PEG<sup>n</sup> (9:1) with n=350, 1000 and 5000 were introduced into the thermostated sample cell of a Nicomp Model 380 Submicron Particle Sizer (PSS, CA, USA), using a 632.8 nm laser source at a fixed scattering angle of 90°. Each sample was measured at least twice for ten minutes. The solvent (distilled D<sub>2</sub>O) was filtrated through regenerated cellulose Amicom Ultra (Millipore, Billerica, MA, USA) filters with 10000 MWCO to eliminate contaminant particles. Data were collected and analyzed with the software provided with the instrument, which utilizes the NICOMP algorithm for diameter calculations. The channel width was automatically set by the instrument and the refraction index and viscosity of the solvent was obtained from literature.

## Results and Discussion

The general structure of the three PE-PEG<sup>n</sup> used is summarized in Fig.1.

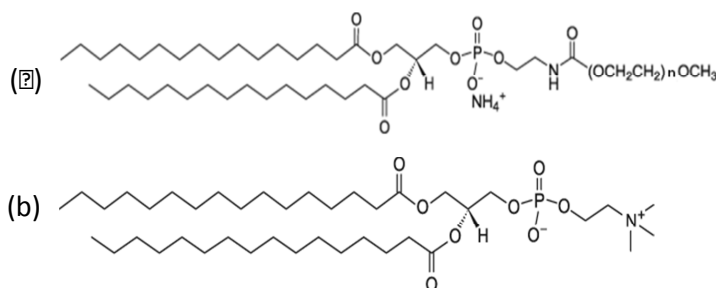


Fig. 1. (a) Molecular Structure of PEG grafted phospholipid. 1,2-dipalmitoyl-sn-glycero-3-phosphoethanolamine-N-metoxi(polyethyleneglycol) (PE-PEG).  $n$  is the molecular mass of PE-PEG<sup>n</sup> (350 Da (PE-PEG<sup>350</sup>), 1000 Da (PE-PEG<sup>1000</sup>), and 5000 Da (PE-PEG<sup>5000</sup>)) with 7, 23 or 113 ethylen(glycol) units, respectively. (b) dpPC structure (1,2-dipalmitoyl-sn-glycero-3-phosphoethanolamine).

PE-PEG<sup>350</sup> is the smallest of the three biopolymers analyzed, with a molecular weight (MW) of 1075.4 Da. From the three PE-PEG derivatives studied, PE-PEG<sup>350</sup> is the most similar to a phospholipid and has the least significant contribution to the molecular density (crowding) of the hydrophilic layer formed by the PEG moiety at the interfacial region of mixed vesicles. In the case of PE-PEG<sup>1000</sup> (MW = 1736.18 Da) the volume ratio between the polar head group (PH) and the hydrophobic hydrocarbon chain (HC) regions are quite balanced, providing a higher molecular density in the hydrophilic layer formed by PEG with some extension parallel to the membrane normal. PE-PEG<sup>5000</sup> is the most massive lipopolymer used in this study (MW = 5745 Da). The high ratio between the size of its PH and the HC suggests a detergent-like behavior<sup>34</sup>. However, contrary to what would be expected, the pure compound is able to form stable monolayers at the air-water interface<sup>35</sup>.

Field Code Changed

Field Code Changed

Here it is also stabilized in the mixture with dpPC. The big size of the PEG moiety in his molecule precludes a high molecular density in the hydrophilic layer.

## <sup>1</sup>H NMR

The <sup>1</sup>H NMR spectra for dpPC/PE-PEG<sup>n</sup> systems are depicted in Fig.2.

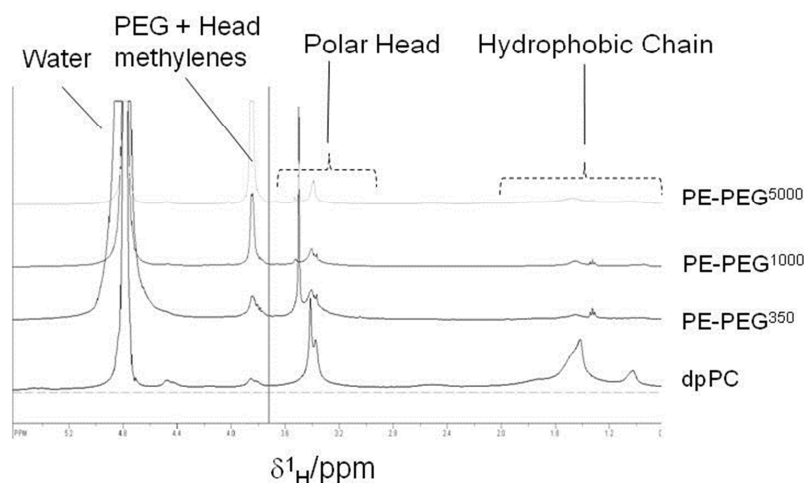


Fig.2. <sup>1</sup>H-NMR spectra of D<sub>2</sub>O dispersions of dpPC/PE-PEG<sup>n</sup> with  $n = 50, 1000$  or  $5000$ . Proton signals have been divided in four regions for better comprehension and to perform the integrals in the inversion-recovery experiments: the signal of residual water at 4.8 ppm, polar head (PH) of dpPC, hydrophobic tail (HC) of dpPC, PEG region overlapped with the head methylenes.

There, we show the assignment of <sup>1</sup>H signals coming from phospholipid and lipopolymer moieties named HC (within 0.8-1.9 ppm), PH (in the region of 3.2-3.6 ppm) and PEG (at 3.8 ppm), together with the signal at 4.8 ppm corresponding to H<sub>2</sub>O, which was present in trace amounts. In the inversion-recovery experiments, each region was integrated separately to obtain the normalized <sup>1</sup>H magnetization,  $M(t)$ , as a function of  $t$ . These  $M_X(t)$  curves followed a bi-exponential behavior,

$$M_X(t) = M_0(1 - 2 \cdot A \cdot \exp(-t/T_{1A}) - 2 \cdot (1-A) \cdot \exp(-t/T_{1B})) \quad [4]$$

where  $X$  is referred to HC, PH, PEG and  $H_2O$ . The parameters  $A$  and  $(1 - A)$  can be directly interpreted as the proportions of each  $T_1$  population sample. In the case  $A=1$ , the fitted function resulted mono-exponential, exhibiting only one relaxation time. Fig.3 displays the experimental data of  $\ln(1-M_X(t)/M_0)$  and the corresponding fittings of eq. 4, for the dpPC/PE-PEG<sup>1000</sup> mixture.

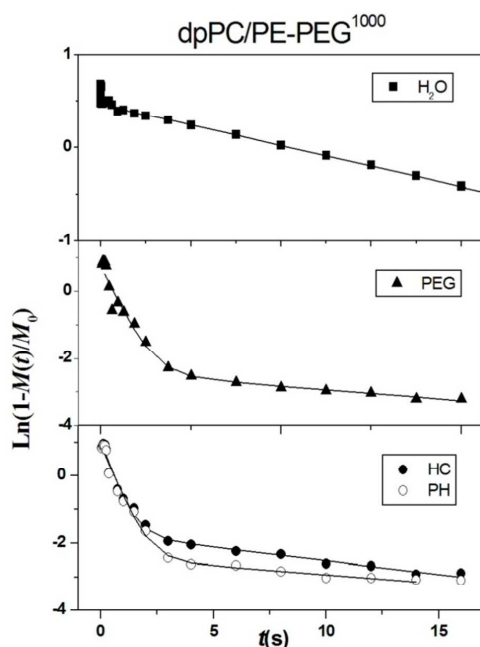


Fig. 3. <sup>1</sup>H Magnetization data of the inversion-recovery experiment as a function of time,  $\ln(1-M(t)/M_0)$ , and the corresponding fittings to eq(1) for mixed dpPC/PE-PEG<sup>1000</sup> vesicles.  $M_{H_2O}$  is shown at the top,  $M_{PEG}$  in the middle and  $M_{HC}$ ,  $M_{PH}$  are shown together at the bottom.

In all the species and molecular moieties analyzed, our results showed the presence of two <sup>1</sup>H populations with long ( $T_{1A}$ ) and short ( $T_{1B}$ ) relaxation times, respectively. Table 1 summarizes the relaxation times  $T_{1A}$  and  $T_{1B}$  and Table 2 summarizes the proportion of <sup>1</sup>H- $T_{1B}$  population in each chemical species or residue analyzed ( $P^B$ ).

**Table 1.**  $^1\text{H}$  - $T_1$  values ( $T_{1A}$  and  $T_{1B}$ ) obtained from a two-exponential fittings performed to  $M(t)$  of the inversion recovery experiments for the systems dpPC/PE-PEG<sup>n</sup>, for all the regions resolved in  $^1\text{H}$  spectra.

Chemical Group	$^1\text{H}$ - $T_1$ (s)					
	dpPC/PE-PEG <sup>350</sup>		dpPC/PE-PEG <sup>1000</sup>		dpPC/PE-PEG <sup>5000</sup>	
	$T_{1A}$	$T_{1B}$	$T_{1A}$	$T_{1B}$	$T_{1A}$	$T_{1B}$
H <sub>2</sub> O	16.8	0.22	18.1	0.19	20	0,03
HC	9.5	0.24	13	0.53	19	0.67
PH	8.4	0.29	17	0.63	19	0.66
PEG	33	0.26	20	0.68	-	0.86

**Table 2.**  $^1\text{H}$  proportions associated to  $T_{1B}$  for all the regions resolved in the  $^1\text{H}$  spectra for the systems dpPC/PE-PEG<sup>n</sup>, obtained from two-exponential fittings performed to  $M(t)$  in the inversion-recovery experiments.

Chemical Group	$P_B$ (proportion of $T_{1B}$ )		
	dpPC/PE-PEG <sup>350</sup>	dpPC/PE-PEG <sup>1000</sup>	dpPC/PE-PEG <sup>5000</sup>
H <sub>2</sub> O	0.26	0.17	0.12
HC	0.92	0.92	0.95
PH	0.92	0.94	0.95
PEG	1	0.93	1

In our system, long relaxation times were in the order of 16.8 -20 s for water, around 20-30 s for PEG and in the range of 8-19 s for PH and HC. In contrast, short relaxation times were found in the range of 0.03-0.22 s for water, while for PEG, PH and HC the values were between 0.24-0.86 s (Table 1). A  $T_1$  of 22 s corresponding to pure water, has been measured previously<sup>36</sup>.

Field Code Changed

Fig.4 is a comparative plot of the long and short relaxation times ( $T_{1A}$  and  $T_{1B}$ ) for the different components involved in the mixture. Note that the larger fitting errors for  $T_1$  values

Formatted: Not Highlight

always appear in the case of the component with the smallest proportion, that is, B component in water and A component for the solid parts (PEG, HC, PH), (see Table 2).

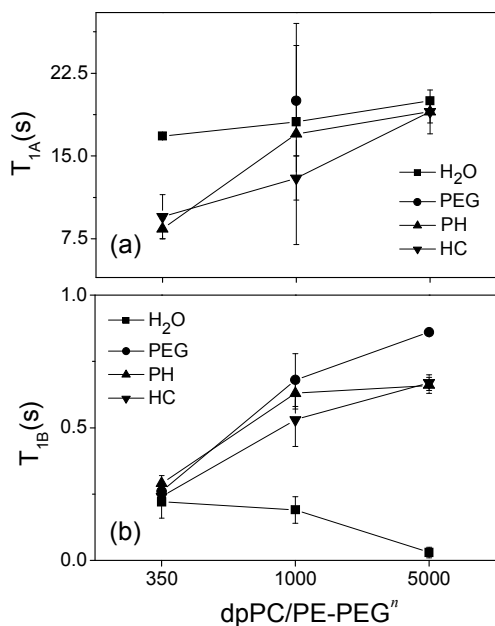


Fig. 4. Long and short relaxation time values in PEGylated phospholipids, as a function of PEG chain length,  $n$ , obtained by fitting a two-exponential function to the magnetization ( $M_X(t)$ ) where  $X$  is H<sub>2</sub>O, PEG, HC, PH. (a) Long relaxation times,  $T_{1A}$ , (b) short relaxation times,  $T_{1B}$ .

Longitudinal (spin-lattice) relaxation times, are related to the correlation times associated to a particular motion.  $T_1$  is also dependent on the Larmor frequency (in our case, 400 MHz) and the strength of the interactions of the local fields<sup>31</sup>. In particular, in the extreme narrowing condition valid for mobile solutions,  $T_1$  is inversely proportional to the motional correlation times. In that limit,  $T_1$  values are decreasing when the fluctuation



1  
2  
3  
4  
5  
6  
7 correlation time increases (i.e. more viscous solutions), while far from this condition  $T_1$   
8 increases with the fluctuations correlation time<sup>31</sup>.

Field Code Changed

9  
10  $T_{1A}$  of water is associated to the faster dynamics while for  $T_{1B}$  of water is related to  
11 slower molecular motion. We can see from Fig.4 and Table 1 that  $T_{1A}$  values for water  
12 increase with  $n$ . Taking into account the mentioned dependence of  $T_1$  with correlation times  
13 for mobile solutions, this behavior is indicative of a decreasing viscosity and faster molecular  
14 mobility of water in suspensions containing lipopolymers with longer PEG moieties. <sup>31</sup>P-  
15 NMR 1D spectra provided a hypothesis to explain this behavior (see below). In contrast,  $T_{1B}$   
16 values corresponding to water showed a decreasing tendency as a function of the size of PEG  
17 moiety reflecting a motion restriction which grows with  $n$  and may be ascribed to confined  
18 water molecules. Interestingly, the proportion  $P^B$  of immobilized water decreases with  $n$   
19 (Table 2). This may be explained by a reduction in the size of the compartment containing the  
20 pool of confined water.  
21  
22  
23  
24  
25  
26  
27  
28  
29  
30

31  
32 Upon comparing  $T_{1A}$  values for PH and HC moieties in the three PE-PEG<sup>n</sup>, it can be  
33 observed a slight increase with  $n$  (Fig. 4a) with values remaining similar between one another  
34 if considered within the same lipopolymer. The later indicates that the phospholipid  
35 components in a lipopolymer are strongly connected and belong to the same proton system.  
36  $T_{1A}$  component for PEG moiety with  $n = 350$  and  $1000$  have values significantly higher than  
37 those of HC and PH in the same compound and followed the opposite tendency decreasing  
38 with  $n$ . This suggests that PEG moiety behaves almost independently with respect to the  
39 phospholipid part of the lipopolymer. In PE-PEG<sup>5000</sup> it was not possible to resolve a bi-  
40 exponential behaviour for PEG. It is important to note that  $T_{1A}$  for PEG, PH and HC  
41 exhibited the lowest contribution to the total spin-lattice relaxation time ( $P_{1A}$ ) (Table 2).  
42  
43  
44  
45  
46  
47  
48  
49  
50

51 The short relaxation time,  $T_{1B}$ , is the component of the spin-lattice relaxation time  
52 most populated ( $P_{1B} > P_{1A}$ ) in PEG as well as in PC and PH residues in phospholipids (Table  
53  
54

1  
2  
3  
4  
5  
6  
7 2).  $T_{1B}$  values for the less mobile components (PEG, PH and HC) follow the same increasing  
8 tendency with  $n$ . This is indicative of a widening in fluctuations within phospholipids and  
9 PE-PEG $n$  molecules in the self-aggregating structures containing lipopolymers. The increase  
10 in  $n$  can be associated with molecules with more pronounced cone-shape and stronger  
11 tendency to self-aggregate in structures of higher surface curvature and lower molecular  
12 packing. This is a consequence of geometrical constraints and steric restrictions that lead to  
13 packing tensions. The later are relieved through a decrease in particles size and an increase in  
14 surface curvature up to the point of changing the type of self-assemble (from bilayer to  
15 micelle) (see below  $^{31}\text{P}$  NMR data). The smallest structures are expected to have the lowest  
16 molecular packing, mainly within the outer leaflet in bilayers<sup>37</sup>. In PE-PEG<sup>350</sup>,  $T_{1B}$  values for  
17 all the components (PEG, PH and HC) are around 0.24-0.29 s. This behavior is probably due  
18 to the strong connections in PE-PEG<sup>350</sup> system that behaves very similar to dpPC creating a  
19 homogeneous environment. On the contrary, for  $n = 5000$  PEG  $T_{1B}$  value (0.86 s) differs  
20 from those of HC (0.67 s) and PH (0.66 s).  
21  
22  
23  
24  
25  
26  
27  
28  
29  
30  
31  
32

33 Recently, from NMR measurements of spin-lattice relaxation times ( $T_1$ ) in PEG<sup>6000</sup>  
34 water solutions, we reported the presence of two molecular populations, both in water and in  
35 PEG as well as a PEG<sup>6000</sup> aggregation also supported by dynamic light scattering data<sup>24</sup>. In  
36 the present work, the existence of two dynamical contributions to the system could be  
37 explained either by an equilibrium between two molecular conformations (phase  
38 coexistence), or by the presence of different types of supramolecular aggregates. The  
39 transition between liposomes and micelles as a function of PEG size and concentration, with  
40 the apparition of disk-like micelles and coexistence of liposomes and micelles have been  
41 studied recently<sup>29, 38</sup>.  
42  
43  
44  
45  
46  
47  
48  
49  
50

51 In order to explore both possibilities explained above, we firstly performed  $^{31}\text{P}$ -NMR  
52 spectra and DLS experiments in aqueous suspensions, and  $\pi$ -Mma compression isotherms  
53  
54

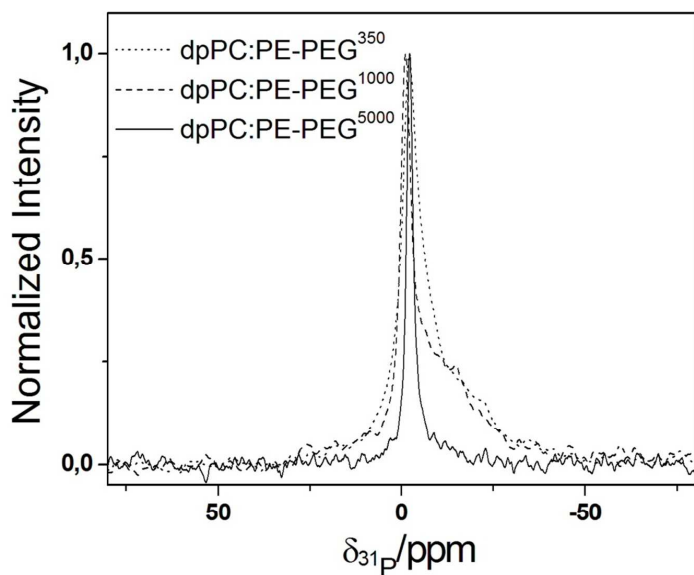
1  
2  
3  
4  
5  
6  
7 and EFM experiments in Langmuir films for all the systems.  
8  
9

### 10 11 12 **<sup>31</sup>P-NMR** 13

14 <sup>31</sup>P-NMR is a powerful technique to explore biomembranes and model systems.  
15  
16 Performing <sup>1</sup>H decoupling, the <sup>31</sup>P spectrum is mainly affected by the chemical shift  
17 anisotropy (CSA). In the hypothetical case of motionless, randomly oriented membrane  
18 structures the <sup>31</sup>P spectrum corresponds to a powder pattern generated by adding up spectra  
19 for all possible orientations (inhomogeneous line). In the opposite case, in micelles, the rapid  
20 reorientation in the NMR time scale produces a total average of the anisotropies yielding a  
21 narrow signal, like in the case of nonviscous solutions with an isotropic motion. In the case of  
22 lamellar liposomes and cylindrical structures the spectrum exhibits a characteristic powder  
23 pattern shape with a peak and a shoulder. Then <sup>31</sup>P-NMR can be used to distinguish between  
24 micelles and liposomes aggregates which relies on the fact that a bigger entity (liposome)  
25 produces a wider signal than a smaller micellar particle<sup>17, 39</sup>. In liposomes the chemical shift  
26 anisotropy (CSA) is measured as the width between the low field shoulder and the main high  
27 field peak of the anisotropic spectrum, reflecting the orientation of the phosphate groups in  
28 the bilayer<sup>17, 39, 40</sup>. The CSA value depends on the molecular and intramolecular motional  
29 averaging.  
30  
31  
32  
33  
34  
35  
36  
37  
38  
39  
40  
41  
42

43 Figure 5 shows the one-dimensional (1D) <sup>31</sup>P-NMR spectra for all the systems under  
44 study. For dpPC/PE-PEG<sup>350,1000</sup> a typical shoulder for a bilayer structure is observed, where  
45 the CSA is 20 ppm (2400 Hz) for  $n=350$  and 13 ppm (1600 Hz) for  $n=1000$ . The smaller  
46 value of CSA for  $n=1000$  reflects a stronger motional averaging in comparison with  $n=350$ .  
47 In contrast, for dpPC/PE-PEG<sup>5000</sup> the phosphate shows a quite symmetric peak associated  
48 with a more isotropic motion, indicating the prevailing presence of micelles. These spectra  
49  
50  
51  
52  
53  
54

1  
2  
3  
4  
5  
6  
7 allowed us to discard the coexistence of different types of supramolecular aggregates. The  
8 formation of liposomes and micelles is related to the PEG chain length. Then for  $n=350$  and  
9  
10 1000 the inclusion of PEG confers a cylindrical geometry to the macromolecule favoring the  
11  
12 formation of bilayers, while for  $n=5000$ , the long chain of PEG and the big size of the polar  
13  
14 head group leads to a conical molecular geometry inducing the formation of micelles<sup>34, 41</sup>.  
15  
16 Then in all the cases, the  $^{31}\text{P}$  1D spectra leads to the conclusion that only one kind of particles  
17  
18 is present (micelles or vesicles).  
19  
20  
21  
22



42 Fig. 5.  $^{31}\text{P}$  NMR spectra of mixed vesicles composed of dpPC and 10 mol% of PE-PEG<sup>n</sup>,  
43 where  $n=350, 1000$  or  $5000$ , dispersed in  $\text{D}_2\text{O}$ .  
44  
45  
46  
47

48 Assuming a smaller size for micelles compared with bilayer vesicles, it may be  
49 expected a lower viscosity for dispersions of particles containing PE-PEG<sup>5000</sup> (micelles) with  
50 respect to those containing PEGs with  $n=350$  and  $1000$  (bilayers vesicles). Note that viscosity  
51 has been proven to decrease upon lowering the size of the nanoparticles in dispersions above a  
52  
53  
54  
55

concentration threshold<sup>42</sup>. Thus, higher  $n$  would correlate with lower particle size (Fig.5) and lower viscosity<sup>42</sup> and would explain the increase in  $T_{1A}$  for water as a function of  $n$  (Fig.4a).

Phase transitions within the polymer regions and phase coexistence within the membrane plane may explain the different  $T_1$  components found in PH, PC and PEG moieties in lipidic molecules.

### EFM and $\pi$ -Mma isotherm

In order to gain a further insight into the behavior of the dpPC/PE-PEG<sup>n</sup> mixtures an

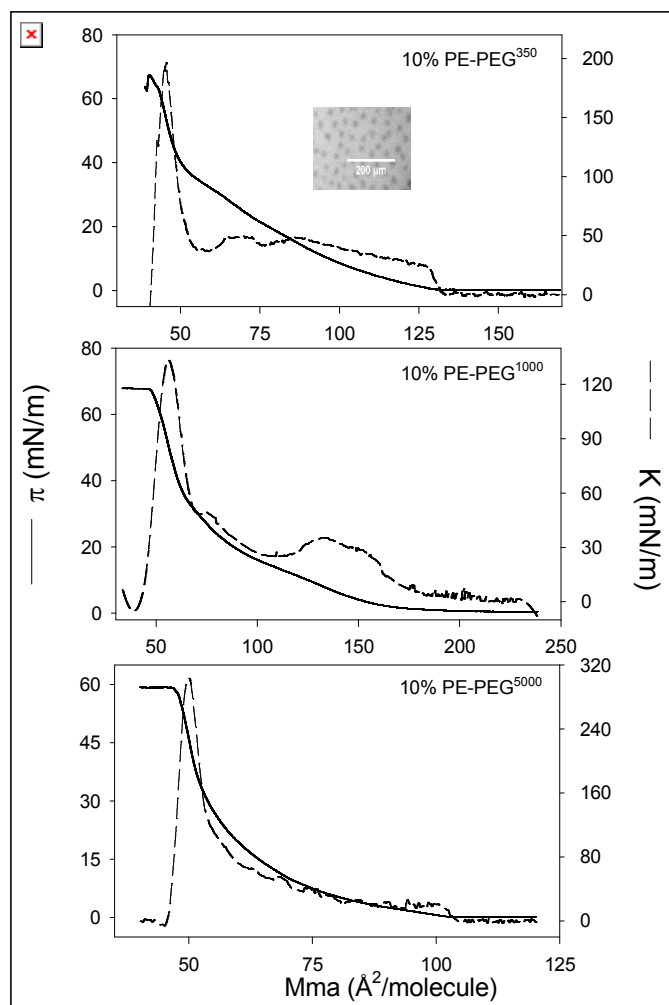


Fig. 6.  $\pi$ -A isotherms for 9:1 binary mixtures of dpPC/PE-PEG<sup>n</sup>, with  $n=350$  (a), 1000 (b) or 5000 (c), respectively. Compressibility modulus (dashed lines) for each compression isotherm, and accompanied with 3 epifluorescence micrographs at different lateral pressures 5, 15 and 35 mN/m.

1  
2  
3  
4  
5  
6  
7 analysis of  $\pi$ -A isotherm is included. Moreover, EFM on Langmuir monolayers of the  
8  
9 mixtures was performed. The  $\pi$ -Mma isotherms, at  $37 \pm 1$  °C, from the 9:1 mixtures of dpPC  
10  
11 with PE-PEG<sup>n</sup> with  $n= 350, 1000$  and  $5000$ ) are shown in Fig.6.

12  
13  
14 The mixtures containing PE-PEG<sup>350</sup> and PE-PEG<sup>1000</sup> exhibit a smooth shape in their  $\pi$ -  
15  
16 Mma and K-Mma isotherms which is in accordance with the homogeneous aspect of the EFM  
17  
18 images at 5 mN/m. Upon rising the lateral pressure, it appears two transitions referred to as t1  
19  
20 and t2 in Fig.6. They correlate with minima in K-Mma isotherms and with the presence of  
21  
22 condensed domains at the interface exhibited by the EFM images. While t1 becomes  
23  
24 completed at  $\sim 19$  mN/m and  $15$  mN/m for PE-PEG<sup>350</sup> and PE-PEG<sup>1000</sup>, respectively, t2 is  
25  
26 observed at higher  $\pi$  (at  $33$  and  $30$  mN/m, respectively) (Figs.6a and 6b). In the film  
27  
28 containing PE-PEG<sup>5000</sup>, the whole  $\pi$ -Mma isotherm looks smooth until the collapse pressure  
29  
30 at  $58$  mN/m. Neither the compressional modulus detects a slope change in the  $\pi$ -Mma  
31  
32 isotherm nor the EFM exhibits condensed domains typically due to phase coexistence.  
33  
34 However, the rough image may reflect molecular aggregates fixed at the interface coming  
35  
36 from a partial collapse of the monolayer (Fig.6c). At  $58$ - $60$  mN/m the collapse of all  
37  
38 monolayers was at a surface pressure compatible with the collapse of an excess of pure dpPC.

39  
40 To understand these results it is important to recall that the  $\pi$ -A isotherms of pure  
41  
42 dpPC at  $30$ - $40$ °C exhibit a 2D transition at  $\pi \sim 20$ - $30$  mN/m characteristic of the liquid  
43  
44 expanded-liquid condensed 2D-phase transition<sup>43, 44</sup>. On the other hand, pure PE-PEG<sup>n</sup>  
45  
46 lipopolymers with  $n \geq 1000$ , at a low molecular packing have been shown to have their  
47  
48 polymeric tails lying at the air-water interface (pancake conformation) which desorbs from the  
49  
50 interface at  $\pi \sim 6$  mN/m acquiring a random coil conformation (mushroom). At  $\sim 30$  mN/m,  
51  
52 lipopolymers with  $n \leq 1000$  suffers another conformational transition within the polymeric  
53  
54 tails towards a stretched conformation (brush), which is driven and stabilized by interactions  
55

1  
2  
3  
4  
5  
6  
7 within the hydrocarbon chains<sup>45, 46</sup>. Both conformations can be achieved by PEGylated  
8 lipopolymers, within certain compositional ranges, in mixed liposomes containing other  
9 phospholipids<sup>47</sup>. The mushroom-brush transition has been shown to occur at a 0.22 PE-  
10 PEG<sup>350</sup> molar fraction and at 0.03 molar fraction of PE-PEG<sup>5000</sup> in mixtures containing these  
11 lipopolymers.  
12  
13  
14  
15

16 Taking together these information, it can be concluded that the mixed monolayers of  
17 dpPC and PE-PEG<sup>n</sup> do not show the pancake – mushroom transition (Fig.6). While t1 in  
18 lipopolymers with  $n = 350$  and 1000 can be ascribed to a 2D-phase transition within  
19 segregated dpPC, t2 may be associated with a mushroom-brush transition within the  
20 polymeric tails of PE-PEG<sup>350,1000</sup>. The absence of a 2D-phase transition in the mixture  
21 containing PE-PEG<sup>5000</sup> indicates the mixed condition of the components at low lateral  
22 pressure and an impairment of the hydrocarbon chains condensation due to a steric hindrance  
23 imposed by the bulky polymeric moiety.  
24  
25  
26  
27  
28  
29  
30

31 The actual PC/PE-PEG<sup>n</sup> molar ratio in the monolayers is expected to be the same as that of  
32 the initial solution spread over the air-water interface. However, a destabilization  
33 phenomenon might be induced at high lateral compression (higher  $\pi$ ) and high temperatures,  
34 leading to a loss of monolayer components and possibly a change in the molecular  
35 composition of the interface. Moreover, the lift-off area (LOA) should increase with the  
36 molecular weight of PEG. This behavior was followed up in mixtures containing PE-PEG<sup>350</sup>  
37 to PE-PEG<sup>5000</sup> at 25°C (not shown) but at 37°C (present work) the LOA of dpPC/PE-PEG<sup>n</sup>  
38 followed the sequence 130, 170 and 120 Å<sup>2</sup>/mole for  $n = 350, 1000$  and 5000. The breaking  
39 of the upward tendency in the value of LOF suggests a particular unstable behavior and the  
40 loss of monolayer in samples containing PEG<sup>5000</sup> (Fig.7, panel c). Then, the increase in  
41 temperature may be the main contributor to the loss of area in this sample. At present, we are  
42 not able to evaluate the final monolayer composition. However, it is interesting to note that  
43  
44  
45  
46  
47  
48  
49  
50  
51  
52  
53  
54

1  
2  
3  
4  
5  
6  
7 the behavior of dpPC/PE-PEG<sup>5000</sup> in the monolayer phase reflects the tendency of molecules  
8 to escape from the planar organization which is consistent with molecules in aqueous  
9 suspension preferring to form self-aggregating structures with high curvature (micelle) as  
10 shown by <sup>31</sup>P-NMR data.  
11  
12  
13

## 14 15 16 17 DLS

18  
19 A DLS analysis of all dispersions was performed and particle size distribution was  
20 analyzed by number, by volume and by intensity. Results are depicted in Fig.7.  
21

22  
23 In samples containing PEG<sup>350</sup> we found three peaks (identified as 1, 2 and 3)  
24 corresponding to particles with average diameters within 25 (20-30) nm, 90 (60-120) nm and  
25 600 (400-900) nm, respectively. Peak 1 was significantly more abundant than the other two  
26 ones. Peak 3 was represented by a very small amount of big particles as indicated by the fact  
27 that it could only be detected through the analysis by volume and not by number. According  
28 to the order of magnitude of the average diameters found, it can be suggested that peaks 1 and  
29 2 might be due to small (SUVs) and large unilamellar vesicles (LUVs) and peak 3 to  
30 multilamellar vesicles (MLVs). The later is consistent with data obtained through SAXS and  
31 TEM experiments with aqueous dispersions of HSPC/PEG400 mixtures<sup>48</sup>.  
32  
33

34  
35 In dpPC/PEG<sup>1000</sup> and dpPC/PEG<sup>5000</sup> samples only Peaks 1 and 2 could be identified.  
36 In these samples, the contribution of Peak 2 to the relative volume was more significant than  
37 in dpPC/PEG<sup>350</sup> samples. According to <sup>31</sup>P NMR data, peak 1 in dpPC/PEG<sup>5000</sup> samples in  
38 the present work is expected to be due to micellar particles exhibiting a size smaller than that  
39 reported in the literature for disk-like micelles present in non-sonicated dpPC/8.3 mole% PE-  
40 PEG<sup>5000</sup> samples.<sup>29</sup> Peak 2 in dpPC/PEG<sup>5000</sup> may include structures containing a bilayer  
41 phase (bicelles or vesicles) in a very small proportion that justifies the slight asymmetry of  
42 the <sup>31</sup>P spectrum recorded in this sample.  
43  
44  
45  
46  
47  
48  
49  
50  
51  
52  
53  
54



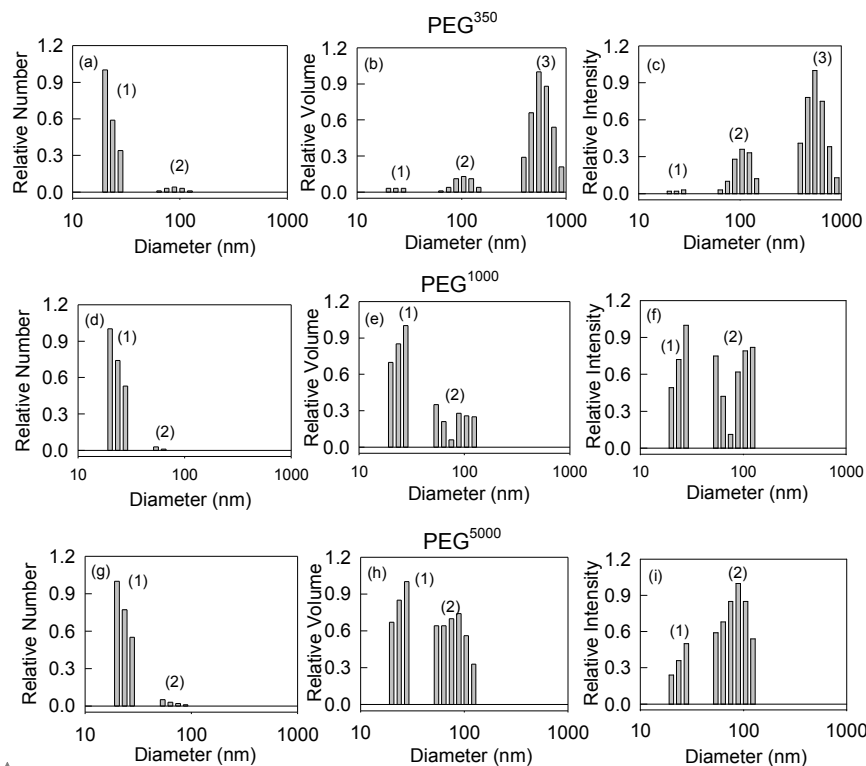


Fig. 7. DLS analysis, by number (a,d,g), by volume (b,e,h) and by intensity (c,f,i) of 9:1 binary mixtures of dpPC/PE-PEG<sup>n</sup>, with  $n=350$  (a,b,c), 1000 (d,e,f) or 5000 (g,h,i), respectively. Three peaks (1,2,3) were identified according to their diameter size. Note that intensity should be the less affected by the "degree of ill-conditioning" in the inversion of the Laplace transform of measured data<sup>49</sup>.

## CONCLUSIONS

In this work we have studied molecular crowded systems modeled by suspensions of binary mixes (9:1) of dpPC and PE modified with PEG having different chain sizes.

1  
2  
3  
4  
5  
6  
7 Performing  $^1\text{H}$  NMR spin-lattice relaxation times measurements with spectral resolution we  
8 could distinguish two  $^1\text{H}$  populations in each component of the solute (PEG and  
9 phospholipids) and the solvent (water), having very different  $T_1$  values, leading to the  
10 possibility of phase coexistence (micelles with liposomes) or different interfacial domains.  
11  
12 The tendency of the  $T_1$  values lead to the conclusion that the solvent decreases its viscosity  
13 and the aggregates reduces its size as a function of the PEG chain size.  
14  
15

16  
17  
18  $T_{1A}^{H_2O}$  reports the behavior of the most immobilized water molecules, mainly those  
19 confined in the aqueous compartment of vesicles - also occupied by motion restricted PEG  
20 chains - becomes less abundant (lower  $P_{1A}^{H_2O}$ ) according the particle size decreases or the  
21 particle type changes from vesicle to micelle. In turn,  $T_{1B}^{H_2O}$ , the most populated of both  
22  $T_1^{H_2O}$  components would report the behavior of structured water (molecules tightly bound to  
23 disordered PEG) plus bulk water which is the dispersing media of self-assembling lipid  
24 particles. The dispersion viscosity is expected to decrease with the decreasing size of  
25 dispersed particles. This would overcompensate the increase in the amount of PEG $^n$ -bound  
26 water and explains the increasing  $T_{1B}^{H_2O}$  values as a function of  $n$ .  
27  
28  
29  
30  
31  
32  
33  
34  
35  
36

37  
38  $T_{1A}$  for HC, PH and PEG exhibited low probability (in the case of PEG<sup>5000</sup> it was  
39 almost zero) and the tendency followed was  $T_{1A}^{HC} \sim T_{1A}^{PH} < T_{1A}^{PEG}$ .  $T_{1B}$  for PEG and for the  
40 lipidic regions HC and PH is the most populated of both  $T_1$  for these molecular regions,  
41 behave as a common proton system and increased with  $n$ , although  $T_{1B}^{PEG}$  seems to grow  
42 faster.  
43  
44  
45  
46  
47

48 The measurements of  $^{31}\text{P}$  spectra led to the conclusion that for  $n=350$  and  $1000$   
49 there are liposomes with reduced size and for  $n=5000$  there are almost only micelles. The  
50 distinguishing behavior in  $^1\text{H}$  NMR populations present in PEG, PH and HC regions of  
51 phospholipid and lipopolymer molecules in conjunction with  $^{31}\text{P}$ -NMR spectra allowed us to  
52  
53  
54

1  
2  
3  
4  
5  
6  
7 postulate that they corresponded to the different domains in a bilayer phase in samples  
8 containing lipopolymers with  $n=350$  and 1000. The presence of these domains was confirmed  
9 by EFM in monolayers at around 30 mN/m which is the expected surface pressure present in  
10 bilayers<sup>50</sup>. In the case of dpPC/PEG<sup>5000</sup> both T1s observed for PH and HC moieties might be  
11 represented by different types of self-aggregated structures.  
12  
13  
14  
15

Field Code Changed

16 All these experiments confirmed the sensitivity of NMR technique to study  
17 macromolecular crowded media not only for giving information about water dynamics but  
18 also giving information about the different aggregates phases and conformations.  
19  
20  
21  
22

## 23 ACKNOWLEDGMENTS

24  
25  
26 Authors are members of the Research career of the Consejo Nacional de Investigaciones  
27 Científicas y Técnicas (CONICET) from Argentina. The present work was supported by  
28 grants from Foncyt, CONICET and SeCyT-Universidad Nacional de Córdoba.  
29  
30  
31  
32

Formatted: English (U.S.)

## 33 Reference List

Field Code Changed

- 34  
35  
36  
37  
38  
39  
40  
41  
42  
43  
44  
45  
46  
47  
48  
49  
50  
51  
52  
53  
54
1. Fulton, A. B. How Crowded Is the Cytoplasm? *Cell* **1982**, *30*, 345-347.
  2. Ellis, R. J.; Minton, A. P. Cell Biology: Join the Crowd. *Nature* **2003**, *425*, 27-28.
  3. Zimmerman, S. B.; Trach, S. O. Estimation of Macromolecule Concentrations and Excluded Volume Effects for the Cytoplasm of Escherichia Coli. *J Mol Biol* **1991**, *222*, 599-620.
  4. Chebotareva, N. A.; Kurganov, B. I.; Livanova, N. B. Biochemical Effects of Molecular Crowding. *Biochemistry (Mosc)* **2004**, *69*, 1239-1251.
  5. Ellis, R. J. Macromolecular Crowding: Obvious but Underappreciated. *Trends in Biochemical Sciences* **2001**, *26*, 597-604.
  6. Ellis, R. J. Macromolecular Crowding: An Important but Neglected Aspect of the Intracellular Environment. *Curr Opin Struct Biol* **2001**, *11*, 114-119.
  7. Hall, D.; Minton, A. P. Macromolecular Crowding: Qualitative and Semiquantitative Successes, Quantitative Challenges. *Biochim Biophys Acta* **2003**, *1649*, 127-139.
  8. Ellis, R. J.; Minton, A. P. Protein Aggregation in Crowded Environments. *Biol Chem* **2006**, *387*, 485-497.
  9. Clop, E. M.; Perillo, M. A. Langmuir Films from Human Placental Membranes: Preparation, Rheology, Transfer to Alkylated Glasses, and Sigmoidal Kinetics of Alkaline Phosphatase in the Resultant Langmuir-Blodgett Film. *Cell Biochemistry and Biophysics* **2010**, *56*, 91-107.

10. Huang, T. M.; Hung, H. C.; Chang, T. C.; Chang, G. G. Solvent Kinetic Isotope Effects of Human Placental Alkaline Phosphatase in Reverse Micelles. *Biochem J* **1998**, *330* ( Pt 1), 267-275.
11. Gouverneur, M.; Berg, B.; Nieuwdorp, M.; Stroes, E.; Vink, H. Vasculoprotective Properties of the Endothelial Glycocalyx: Effects of Fluid Shear Stress. *Journal of Internal Medicine* **2006**, *259*, 393-400.
12. Vackier, M.-C.; Hills, B. P.; Rutledge, D. N. An Nmr Relaxation Study of the State of Water in Gelatin Gels. *Journal of Magnetic Resonance* **1999**, *138*, 36-42.
13. Sabadini, E.; Egidio, F. d. C.; Fujiwara, F. Y.; Cosgrove, T. Use of Water Spin-Spin Relaxation Rate to Probe the Solvation of Cyclodextrins in Aqueous Solutions. *J. Phys. Chem. B* **2008**, *112*, 3328-3332.
14. Kuentz, M.; Rothenhäusler, B.; Röthlisberger, D. Time Domain 1h Nmr as a New Method to Monitor Softening of Gelatin and Hpmc Capsule Shells. *Drug Dev Ind Pharm* **2006**, *32*, 1165-1173.
15. Demangeat, J.-L. Nmr Water Proton Relaxation in Unheated and Heated Ultrahigh Aqueous Dilutions of Histamine: Evidence for an Air-Dependent Supramolecular Organization of Water. *Journal of Molecular Liquids* **2009**, *144*, 32-39.
16. Wilkinson, D. A.; Morowitz, H. J.; Prestegard, J. H. Hydration of Phosphatidylcholine. Adsorption Isotherm and Proton Nuclear Magnetic Resonance Studies. *Biophysical Journal* **1977**, *20*, 169-179.
17. Leal, C. I.; RÅngvaldsson, S.; Fossheim, S.; Nilssen, E. A.; Topgaard, D. Dynamic and Structural Aspects of Pegylated Liposomes Monitored by Nmr. *Journal of Colloid and Interface Science* **2008**, *325*, 485-493.
18. Triba, M. N.; Warschawski, D. E.; Devaux, P. F. Reinvestigation by Phosphorus Nmr of Lipid Distribution in Bicelles. *Biophys.J.* **2005**, *88*, 1887-1901.
19. Farruggia, B.; Nerli, B.; Pico, G. Study of the Serum Albumin-Polyethyleneglycol Interaction to Predict the Protein Partitioning in Aqueous Two-Phase Systems. *J Chromatogr B Analyt Technol Biomed Life Sci* **2003**, *798*, 25-33.
20. Pico, G.; Romanini, D.; Nerli, B.; Farruggia, B. Polyethyleneglycol Molecular Mass and Polydispersity Effect on Protein Partitioning in Aqueous Two-Phase Systems. *J Chromatogr B Analyt Technol Biomed Life Sci* **2006**, *830*, 286-292.
21. Elbert, D. L.; Hubbell, J. A. Surface Treatments of Polymers for Biocompatibility. *Annual Review of Materials Science* **1996**, *26* 365-294.
22. de Gennes, P. G. Conformations of Polymers Attached to an Interface. *Macromolecules* **1980**, *13*, 1069-1075.
23. Lee, J. H.; Lee, H. B.; Andrade, J. D. Blood Compatibility of Polyethylene Oxide Surfaces. *Progress in Polymer Science* **1995**, *20* 1043-1079.
24. Clop, E. M.; Perillo, M. A.; Chattah, A. K. <sup>1</sup>h and <sup>2</sup>h Nmr Spin-Lattice Relaxation Probing Water: Peg Molecular Dynamics in Solution. *J Phys Chem B* **2012**, *116*, 11953-11958.
25. Schneider, M. F. Forces, Thermodynamics and Structure of Artificial Glycocalyx Models in Two and Three Dimensions. Technische Universitat Munchen, 2003.
26. Schneider, M. F.; Lim, K.; Fuller, G. G.; Tanaka, M. Rheology of Glycocalix Model at Air/Water Interface. *Physical Chemistry Chemical Physics* **2002**, *4*, 1949-1952.
27. Kim, J. Y.; Kim, J. K.; Park, J. S.; Byun, Y.; Kim, C. K. The Use of Pegylated Liposomes to Prolong Circulation Lifetimes of Tissue Plasminogen Activator. *Biomaterials* **2009**, *30*, 5751-5756.
28. Woodle, M. C.; Lasic, D. D. Sterically Stabilized Liposomes. *Biochim Biophys Acta* **1992**, *1113*, 171-199.

29. Johnsson, M.; Edwards, K. Liposomes, Disks, and Spherical Micelles: Aggregate Structure in Mixtures of Gel Phase Phosphatidylcholines and Poly(Ethylene Glycol)-Phospholipids. *Biophys.J.* **2003**, *85*, 3839-3847.
30. Corvalan, N. A.; Clop, E. M.; Perillo, M. A. In *Surface Behaviour of Dipalmitoyl Phosphatidylethanolamine Grafted Poly(Ethylene Glycol) Alone or in Mixtures with Dipalmitoyl Phosphatidylcholine*, XXXVII Reunión Anual de la Sociedad Argentina de Biofísica, La Plata, Buenos Aires, Argentina, Sociedad Argentina de Biología: La Plata, Buenos Aires, Argentina, 2008.
31. Harris, R. *Nuclear Magnetic Resonance Spectroscopy*. Longman Scientific and Technical: England, 1994; p 250.
32. Turina, A. V.; Caruso, B.; Yranzo, G. I.; Moyano, E. L.; Perillo, M. A. A Surface Active Benzodiazepine Receptor Ligand for Potential Probing Membrane Order of Gabaa-Receptor Surroundings. *Bioconjug Chem* **2008**, *19*, 1888-1895.
33. Clop, E.; Clop, P.; Sánchez, J. M.; Perillo, M. A. Molecular Packing Tunes in the Kinetics of Beta-Galactosidase Catalyzed O-Nitrophenyl Galactopiranoside Hydrolysis. *Langmuir* **2008**, *24*, 10950-10960.
34. Israelachvili, J. N. *Intermolecular and Surface Forces*. Academic Press: New York, 1989.
35. Clop, E. M.; Corvalan, N. A.; Perillo, M. A. Langmuir Films of Dipalmitoyl Phosphatidylethanolamine Grafted Poly(Ethylene Glycol). In-Situ Evidence of Surface Aggregation at the Air-Water Interface. *Coll.Surf.B: Biointerfaces (under revision)* **2013**.
36. Clop, E. M.; Perillo, M. A.; Chatta, A. K. <sup>1</sup>h and <sup>2</sup>h Nmr Spin-Lattice Relaxation Probing Water - Peg Molecular Dynamics in Solutions. *J.Phys.Chem.B* **2012**, *116*, 11953-11958.
37. Garcia, D. A.; Perillo, M. A. Flunitrazepam Induces Geometrical Changes at the Lipid-Water Interface. *Coll.Surf.B: Biointerfaces* **2001**, *20*, 63-72.
38. Georgiev, G. A.; Sarker, D. K.; Al-Hanbali, O.; Georgiev, G. D.; Lalchev, Z. Effects of Poly (Ethylene Glycol) Chains Conformational Transition on the Properties of Mixed Dmpc/Dmpe-Peg Thin Liquid Films and Monolayers. *Coll.Surf.B: Biointerfaces* **2007**, *59*, 184-193.
39. Levstein, P. R.; Gennaro, A. M.; Pincelli, M. M. <sup>31</sup>p-Nmr and Spin Label Epr as Complementary Techniques for Lipid Polymorphism Studies. In *Recent Research Developments in Biophysical Chemistry*, Condat, C. A.; Baruzzi, A. M., Eds. Research Signpost: Kerala, India, 2002.
40. Seelig, J. <sup>31</sup>p Nuclear Magnetic Resonance and the Head Group Structure of Phospholipids in Membranes. *Biochim Biophys Acta* **1978**, *515*, 105-140.
41. Perillo, M. A.; Scarsdale, N. J.; Yu, R. K.; Maggio, B. Modulation by Gangliosides of the Lamellar-Inverted Micelle (Hexagonal Ii) Phase Transition in Mixtures Containing Phosphatidylethanolamine and Dioleoylglycerol. *Proc Natl Acad Sci U S A* **1994**, *91*, 10019-10023.
42. Nguyen, C. T.; Desgranges, F.; Roy, G.; Galanis, N.; Maré, T.; Boucher, S.; Angue Mintsas, H. Temperature and Particle-Size Dependent Viscosity Data for Water-Based Nanofluids – Hysteresis Phenomenon. *Int. J. Heat Fluid Flow* **2007**, *28*, 1492–1506.
43. Toimil, P.; Prieto, G.; Miñones, J. J.; Sarmiento, F. A Comparative Study of F-Dppc/Dppc Mixed Monolayers. Influence of Subphase Temperature on F-Dppc and Dppc Monolayers. *Phys. Chem. Chem. Phys.* **2010**, *12*, 13323–13332.
44. Yun, H.; Choi, Y.-W.; Kim, N. J.; Sohn, D. Physicochemical Properties of Phosphatidylcholine (Pc) Monolayers with Different Alkyl Chains, at the Air/Water Interface. *Bull. Korean Chem. Soc.* **2003**, *24*, 377-383.
45. Milner, S. T. Polymer Brushes. *Science* **1991**, *251*, 905-914.

- 1  
2  
3  
4  
5  
6  
7 46. Lecourtier, J.; Audebert, R.; Quivoron, C. Swelling of Macromolecules Grafted on Inert  
8 Surfaces and Partitioning of a Solute between Solvent and Grafted Phase.  
9 *Macromolecules* **1979**, *12*, 141-146.  
10 47. Marsh, D.; Bartucci, R.; Sportelli, L. Lipid Membranes with Grafted Polymers:  
11 Physicochemical Aspects. *Biochim Biophys Acta* **2003**, *1615*, 33-59.  
12 48. Sakuragi, M.; Koiwai, K.; Nakamura, K.; Masunaga, H.; Ogawa, H.; Sakurai, K.  
13 Transformation from Multilamellar to Unilamellar Vesicles by Addition of a Cationic  
14 Lipid to Pegylated Liposomes Explored with Synchrotron Small Angle X-Ray  
15 Scattering. *Journal of Physics: Conference Series* **2011**, *272*, 012011.  
16 49. De Vos, C.; Deriemaeker, L.; Finsy, R. Quantitative Assessment of the Conditioning of  
17 the Inversion of Quasi-Elastic and Static Light Scattering Data for Particle Size  
18 Distributions. *Langmuir* **1996**, *12*, 2630–2636.  
19 50. Marsh, D. Lateral Pressure in Membranes. *Biochim Biophys Acta* **1996**, *1286*, 183-223.  
20  
21  
22  
23  
24  
25  
26  
27  
28  
29  
30  
31  
32  
33  
34  
35  
36  
37  
38  
39  
40  
41  
42  
43  
44  
45  
46  
47  
48  
49  
50  
51  
52  
53  
54  
55  
56  
57  
58  
59  
60

## Table of Contents Image

